A Physical Model for Predicting Throughput of Wireless LANs

Mostafa Pakparvar, David Plets, Luc Martens, Wout Joseph

Abstract This paper presents an experimentally verified heuristic physical model to predict the throughput of a Wireless LAN link in presence of homogeneous interference of neighboring networks. The model predicts achievable throughput based upon two interference characteristics: transmission rate of the interface and the channel occupancy degree of the interference which is a measure of user activity defined in the paper.

1 Introduction

Large scale growth of wireless networks and spectrum scarcity are introducing more interference than ever. Intensive interference degrades wireless links and may jeopardize seamless connectivity and hence Quality of Service (QoS) offered to the users.

Cognitive Radios (CRs) are becoming a tempting solution to tackle this type of spectrum over-utilization by introducing opportunistic usage of frequency bands that are not heavily occupied by licensed users [1]. The equal regulatory status of wireless terminals on the Industrial Scientific Medical (ISM) band leaves no consideration of a primary user for wireless users. Therefore, interoperability of ISM band networks is becoming a key issue that must be solved.

Wireless networks are designed to tackle homogeneous intra/inter network interference by means of various medium access techniques. The efficiency of interference mitigation techniques of the present technologies has been profoundly assessed in literature. For instance in [2], a large number of experiments prove that the

Mostafa Pakparvar, David Plets, Luc Martens, Wout Joseph
Department of Information Technology (INTEC) - Ghent University - iMinds
Gaston Crommenlaan 8, Box 201, 9050 Gent, Belgium,
e-mail: Mostafa.Pakparvar@intec.ugent.be

throughput of IEEE 802.11 WLAN is highly dependent on the traffic characteristics of other present Wi-Fi networks.

Artificial neural networks (ANN) have also been used for radio parameter adaptation in CR [3, 4]. The ANN determines radio parameters for given channel states with three optimization goals, including meeting the bit error rate (BER), maximizing the throughput and minimizing the transmit power. In [5], it is proposed to use the ANN to characterize the real-time achievable communication performance in CR. Since the characterization is based on runtime measurements, it provides a certain learning capability that can be exploited by the cognitive engine. The simulation results demonstrate good modeling accuracy and flexibility in various applications and scenarios.

Metaheuristics [6] are used for combinatorial optimization in which an optimal solution is sought over a discrete search-space. Evolutionary Algorithms/Genetic Algorithms (GA)s, Simulated Annealing (SA), Tabu Search (TS) and Ant Colony Optimization (ACO) are examples of metaheuristic algorithms. Among the various metaheuristic algorithms, the GA has been widely adopted to solve multiobjective optimization problems and to dynamically configure the CR in response to the changing wireless environment. For instance in [7], Park et al. validate the applicability of GA-based radio parameter adaptation for the CDMA2000 forward link in a realistic scenario with Rician fading. In [8], a GA-based cell-by-cell dynamic spectrum-allocation scheme is investigated achieving better spectral efficiency than the fixed spectrum-allocation scheme. A new solution-encoding technique is proposed to reduce the GA convergence time. In [9], a software testbed for CR with the spectrum-sensing capability is implemented and a GA-based CE to optimize radio parameters for dynamic spectrum access (DSA).

Game theory techniques have also been widely used in the context of cognitive radios. In [10], population game theory has been applied to model the spectrum access problem and develop distributed spectrum access policies based on imitation, a behavior rule widely applied in human societies consisting of imitating successful behaviors. In [11], the authors study the spectrum access problem in cognitive radio networks from a game-theoretical perspective. The problem is modeled as a non-cooperative spectrum access game where secondary users simultaneously access multiple spectrum bands left available by primary users, optimizing their objective function which takes into account the congestion level observed on the available spectrum bands.

Apart from all aforementioned sophisticated methods, there are also methods in literature that derive a physical model for the target parameters based on monitoring physical layer parameters like Received Signal Strength Indicator (RSSI) or Carrier to Interference and Noise Ratio (CINR). For instance, in [12], the authors derive such a physical relation for modeling the throughput of WiMax networks based on the CINR value at the receiver.

In this paper we develop a novel experimentally verified heuristic model to predict and optimize the throughput of wireless terminals in a cognitive network. The model is to be used as the kernel of a cognitive decision engine. The prediction is based on the physical spectrum information. Information is collected passively from

the environment i.e., it does not require any interaction with external/third party networks and resources.

The model is derived from a set of exploratory measurements and is validated with various practical measurements in a pseudo shielded experimental testbed building, w-iLab.t [13]. This paper is organized as follows: in Section 2, the exploratory measurements are described. Section 3, presents the heuristic physical model. Section 4 presents the conclusion of this paper.

2 Exploratory measurements

After describing the network configuration and the experiment setup, we will elaborate the exploratory measurements we performed for deriving the physical model of the throughput.

2.1 Experiment description

2.1.1 Network configuration

All experiments are conducted in a pseudo-shielded testbed environment [13] in Ghent, Belgium. The nodes in the testbed are mounted in an open room (66 m x 20.5 m) in a grid configuration with an x-separation of 6 m and a y-separation of 3.6 m. Figure 1 shows the ground plan of the living lab with an indication of the location of the nodes. Each node has two Wi-Fi interfaces (Sparklan WPEA-110N/E/11n mini PCIe 2T2R chipset: AR9280) and on each Wi-Fi card, two antennas are connected (2x2 MIMO (Multiple-Input Multiple-Output) is supported). Furthermore, a ZigBee sensor node and a USB 2.0 Bluetooth interface (Micro CI2v3.0 EDR) are incorporated into each node.

2.1.2 Experiment setup

In each of the interference measurements, a set of experiments is executed. Each experiment consists of two phases: a first phase where the QoS of the link under test is recorded without interference, and a second phase where interference is generated in the environment. Phase 2 of each experiment proceeds as follows:(i) Start the interference transmission (ii) Wait 1 second to insure interference is on the air (iii) Start the link under test transmission for n seconds (iv) Stop all data transmissions. The value of n is set to 10 by default unless otherwise mentioned. During the execution of an experiment, the Iperf output stream containing the periodic throughput reports of the receiver is parsed and stored in a database at the experiment controller server of the testbed. For each record, we also log the time stamp of the throughput

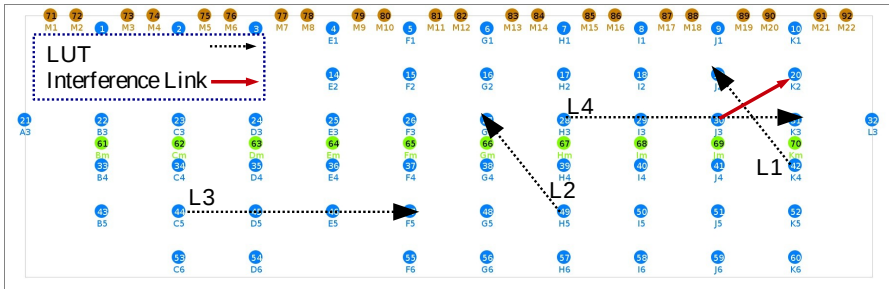

Fig. 1: W-iLab.t living lab test environment (66m x 20.5m) with indication of the nodes and the connection links used for the experiments. Links L1 and L2 are 9.37m long and L3 and L4 are 18m long.

report. Moreover, all physical-layer changes such as channel switching and transmit power modifications together with their time stamps are logged into the database. After running the experiments, the time stamps of the physical- layer changes are used in order to calculate the achieved throughput during each of the experiments in the total set.

During each interference measurement, two connection links are established, as displayed in Figure 1. The first link, always operating on channel 6, is denoted as the link under test (LUT). By default this link is set at the location L1 (see Figure 1) unless otherwise mentioned. The second link is the interfering link, between node 30 and node 20 (see the solid link in Figure 1). The data generation rate of the transmitters is defined as the UDP (User Datagram Protocol) bandwidth of the Iperf application. All Wireless Local Area Network (WLAN) radio interfaces are set to transmit at a certain bit rate (TxRate) and Iperf [14] was used as the traffic generator. The channel occupancy degree (COD) is here defined as the ratio of the data generation rate and the TxRate. There is a transmit buffer that is filled by data at a rate equal to the data generation rate, while the interface transmits through this buffer at a rate equal to the TxRate. The data generation rate is always smaller than or equal to the TxRate.

$$\text{COD}\ [\%] = \frac{\text{Data Generation Rate [Mbps]}}{\text{TxRate [Mbps]}} \times 100 \tag{1}$$

2.2 *Measurement I: Assessment of channel overlap and interference level influence on throughput*

The first measurement studies the influence of channel overlap of the interference link on the throughput of the link under test. This measurement consists of 70 iterations each characterized by the interference channel (5 channels) and by the gen-

erated interference level (14 levels) as observed at node 19 (caused by interfering node 30). The channel of the interfering link was varied from channel 6 (full overlap with link under test) to channel 10 (smallest overlap with link under test). For each channel overlap, fourteen different interference power levels [dBm] were observed at node 19: [-51,-52,-53,-54,-56,-57,-59,-60,-62,-63,-66,-70,-71,-72]. This measurement was repeated for 2, 18, and 48 Mbps TxRates for the case of interference on channel 6 and 7 and for 2, 11, 24, and 48 Mbps TxRates for the case of interference on channel 8, 9, and 10 to see if the TxRate influences the throughput on non-overlapping channels. In all iterations, the transmission rate of the LUT equals that of the interference link and the COD of the interference link is equal to 100% (see Equation 1). The value of n (duration of the assessment) was set to 500 seconds in this measurement.

Figure 2 shows the achieved average throughput as a function of the received interference power level, for interference on different channels. Each region is identified by a bit rate which is the TxRate of the LUT and interference link. Note that here the interference COD is equal to 100%. A higher channel number corresponds with less overlap, i.e., for increasing channel separations, interference decreases (LUT operates on channel 6). The interference level on the x-axis of these Figures is defined as the power received from node 30 at node 19 (see Figure 1).

Measurement results in Figure 2 show that the sensitivity of the throughput to the interference channel overlap depends on the transmission rate of the links. Firstly, the interference power level does not affect the throughput when the interference power level is above a certain TxRate-channel dependent threshold: the throughput is not more impacted when the interference power is higher.

The upper regions of Figure 2 reveal high sensitivity of throughput on interference level and interference transmission rate at higher TxRates. Interference on channels 9 and 10 (channel separation of 3 and 4) affects the throughput only when the interference TxRate is above 2 Mbps. For the 48 Mbps case for instance, there is more than 30% throughput reduction for interference power levels above -70 and -60 dBm on channels 9 and 10 respectively. In all cases, at higher interference TxRates, the interference level is a key parameter that influences the achieved throughput.

Therefore, channel overlap between the interference source and the network under study is an important parameter that affects the throughput of WLANs. The results of these measurements suggest that if the cognitive decision engine has to select an overlapping channel, it should select the channel with the least interference level and has lower interference TxRate.

2.3 Measurement II: Joint assessment of the interference TxRate and interference COD influence on throughput

Since interference COD and interference TxRate are not completely uncorrelated parameters, deriving a decent 2-dimensional model requires joint assessment of the two parameters influence on throughput. Here L3 serves as LUT and the same se-

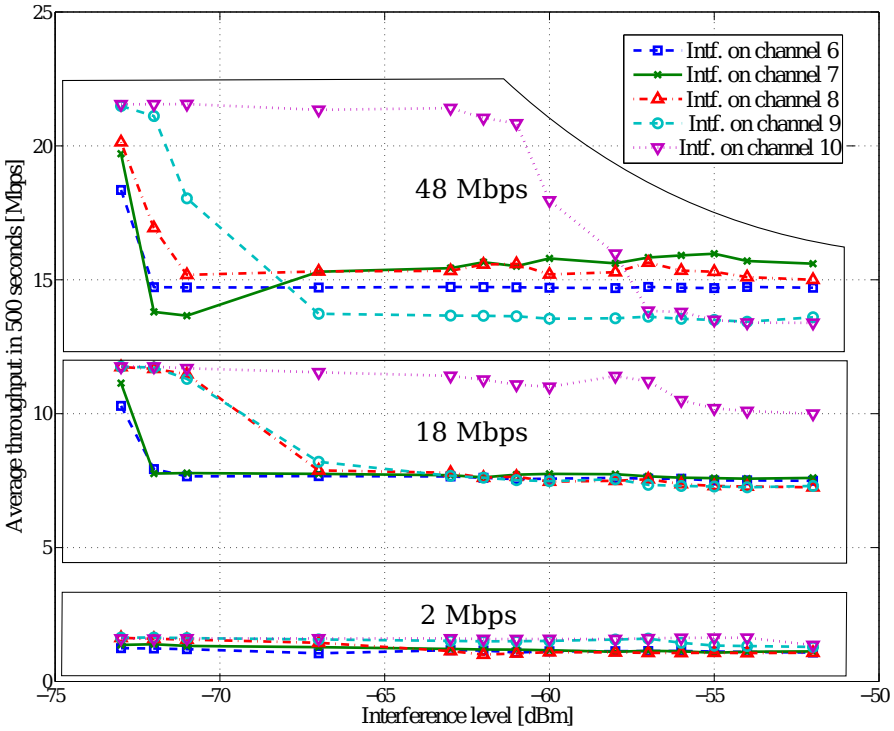

Fig. 2: Average throughput over link under test in a 500 second time frame as a function of received interference power level, for interference with different channel overlaps. Each region has its corresponding TxRate of the LUT and interference link. Intf. COD = 100%. The LUT is on channel 6.

lection of interference link as described in previous measurements is used. We measure the average achievable throughput in a ten seconds interval with interference TxRates of [2 11 18 24 36 48 54] and interference COD values starting from 0 to 100% in steps of 6.25%. All links are set to channel 6 and the transmit power of all terminals is set to 20 dBm. The TxRate of the LUT is set to 54 Mbps and its COD is set to 100% percent such that the maximum achievable throughput is measured.

Sample points in Figure 3 show the results of validation measurement on link L1. Looking at the results of this measurement unveils the dependency of the interference COD and TxRate when predicting the throughput value. This is more investigated in next Section.

3 Development of the Model

3.1 Construction of models

Data transmission rate of the Wi-Fi interface and the user activity are the key parameters that determine the spectrum utilization by any terminal. For a fixed amount of data transmission, higher transmission rate (TxRate) means less spectrum occupancy in time. Hence, an active user with low transmission rate occupies the spectrum to an extent that users of other networks in the vicinity experience a much lower than expected throughput.

The model predicts the achievable throughput (T) based on the interference characteristics. Parameters that characterize the interference are: COD of the interference, interference TxRate, interference frequency channel. All parameters are obtainable using the monitor mode of IEEE 802.11 interfaces [15] and packet tracing applications like libtrace [16] and tcpdump [17]. Extension to all Wi-Fi channels is feasible by periodic monitoring of all channels or by exploiting more WLAN interfaces at different locations of the network each operating on a single channel.

Due to the dependency of the interference parameters, deriving a decent 2-dimensional model to predict the throughput is crucial. The observation of the throughput behavior in sample points of Figure 3 shows that depending on the interference TxRate, the achieved throughput increases exponentially after a certain interference COD threshold. Therefore, by applying unit step function to the exponential models and partitioning the space into linear and exponential regions, we come up with an accurate model. This is evidenced by the results of our suggested model in Equation 2 below:

$$\begin{aligned} T(COD_{Intf.}, TxRate_{Intf.}) = \\ (a_0 e^{-b.COD_{Intf.}})u(90 - COD_{Intf.} - r.TxRate_{Intf.}) + \\ (a_0 e^{-b(90 - r.TxRate_{Intf.})})u(COD_{Intf.} + r.TxRate_{Intf.} - 90) \end{aligned} \quad (2)$$

where u(t) is the unit step function, $TxRate_{Intf.}$ denotes interference TxRate, $COD_{Intf.}$ denotes interference COD, and the coefficient parameters should be optimized for the intended link and the intended channel. The nonlinear least square optimization results for measurements on link L3 assigns an a_0 value of 23.23, $b = 0.02$ and $r = 0.5$. These values are obtained by exploiting all the sample points of the measurement II. Figure 3 illustrates this realization of the model for sample points of link L3. Note that the configuration of the step function arguments are optimized manually by looking up the results of measurement II where threshold of the aforementioned throughput exponential behavior increases linearly from a COD of 90% for TxRate of 2 Mbps up to the COD value of 60% for TxRate of 54 Mbps. The obtained R^2 (coefficient of determination) value is 0.9425 and the Root Mean Square Error (RMSE) value is 1.34 which show the accuracy of the model.

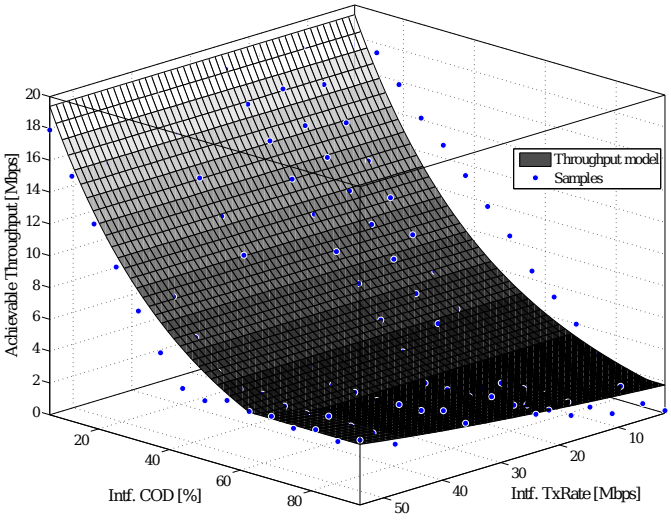

Fig. 3: The 3D demonstration of the throughput model realized at L3.

3.2 Validation measurements

The objective of these measurements is to verify the 2-dimensional model of Equation 2 for different sender-receiver distances and different link locations. To this end, different combinations of LUT terminals with various distances of sender-receiver were used while the interference link was fixed. These links are illustrated in Figure 1: link L2 is a replication of L1 while L4 is a replication of L3 at another location. Except for the LUT terminal locations, the measurement configuration is identical to measurement II described in Section 2.3.

3.3 Validation results

The model obtained by using measurements at link L3 is assessed with measurements on links L1, L2 and L4. The results are reported in Table 1. All R^2 values are above 0.89 and the RMSE does not exceed 1.7 Mbps. The maximum deviation is 3.3 Mbps which is acceptable when compared to the achievable throughput range of 20 Mbps. Hence, the model optimized for a single link location can serve to predict the throughput at other links with an acceptable accuracy. This measurement setup was limited to the node locations and propagation characteristics of the testbed. However, for environments with more diverse propagation characteristics and larger sender-receiver distances, a correction parameter can be added to the model to compensate the throughput drop due to more attenuation. The simplicity of this model enables the decision engine to devise it with a small number of sam-

Table 1: Statistics of the verifying measurements at various links with the model obtained at L3.

Link	RMSE [Mbps]	Max. Deviation [Mbps]	R^2
L4	1.65	3.31	0.8987
L3	1.34	2.93	0.9425
L2	1.59	2.57	0.9056
L1	1.59	2.66	0.9059

ple points. Figure 4 shows the RMSE and R^2 of the model realized with varying number of sample points. Every realization is a set of measurements with all possible $TxRate_{Intf.}$ values and $COD_{Intf.}$ values uniformly distributed between 0% and 100%. The R^2 value is always more than 0.94 and the RMSE is always less than 1.35 Mbps. These statistics show that the model can be devised accurately with 42 samples.

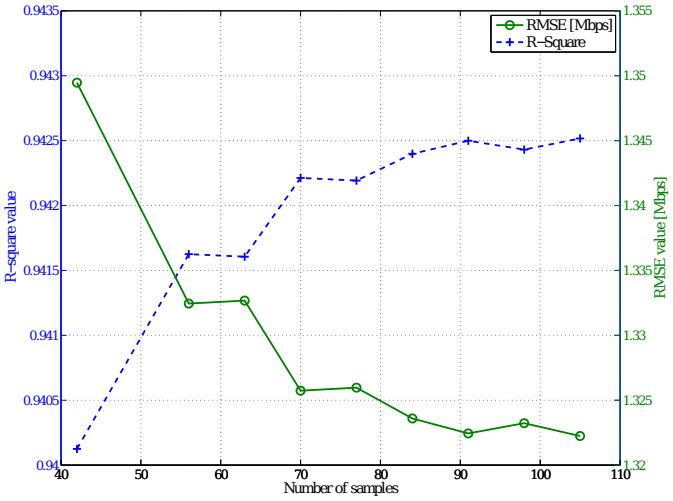

Fig. 4: Statistics of the model for realizations with varying number of sample points.

4 Conclusion and Future work

Based upon numerous exploratory measurements, a novel physical throughput model accounting for interference channel occupancy degree ($COD_{Intf.}$) and interference transmission rate ($TxRate_{Intf.}$) was devised and verified in a pseudo-shielded testlab environment.

Future research on this framework includes comparison of the performance of the cognitive engine based on the proposed model with smarter higher level algorithms, and integration of this type of physical modeling with other decision algorithms to achieve more efficient algorithms. This model was devised in a pseudo-shielded environment, therefore extension to office and industry environments can be the topic of further research.

Acknowledgment

This work was supported by the iMinds-ICON QoCON project, co-funded by iMinds, a research institute founded by the Flemish Government in 2004, and the involved companies and institutions. The research is also partly funded by the Fund for Scientific Research - Flanders (FWO-V, Belgium) project G.0325.11N.

References

1. I. Mitola, J. and J. Maguire, G.Q., "Cognitive radio: making software radios more personal," *IEEE Personal Communications*, vol. 6, pp. 13 –18, Aug. 1999.
2. D. Plets, M. Pakparvar, W. Joseph, and L. Martens, "Influence of intra-network interference on quality of service in wireless lans," in *Proc. IEEE International Symposium on Broadband Multimedia Systems and Broadcasting (BMSB'2013)*, June 2013.
3. M. Hasegawa, H.-N. Tran, G. Miyamoto, Y. Murata, and S. Kato, "Distributed optimization based on neurodynamics for cognitive wireless clouds," in *IEEE 18th International Symposium on Personal, Indoor and Mobile Radio Communications, 2007. PIMRC 2007*, pp. 1–5, 2007.
4. Z. Zhang and X. Xie, "Intelligent cognitive radio: Research on learning and evaluation of CR based on neural network," in *ITI 5th International Conference on Information and Communications Technology, 2007. ICICT 2007*, pp. 33–37, 2007.
5. N. Baldo and M. Zorzi, "Learning and adaptation in cognitive radios using neural networks," in *Consumer Communications and Networking Conference, 2008. CCNC 2008. 5th IEEE*, pp. 998–1003, 2008.
6. C. Blum and A. Roli, "Metaheuristics in combinatorial optimization: Overview and conceptual comparison," *ACM Comput. Surv.*, vol. 35, pp. 268–308, Sept. 2003.
7. S. K. Park, Y. Shin, and W. C. Lee, "Goal-pareto based nsga for optimal reconfiguration of cognitive radio systems," in *Cognitive Radio Oriented Wireless Networks and Communications, 2007. CrownCom 2007. 2nd International Conference on*, pp. 147–153, 2007.
8. D. Thilakawardana and K. Moessner, "A genetic approach to cell-by-cell dynamic spectrum allocation for optimising spectral efficiency in wireless mobile systems," in *Cognitive Radio Oriented Wireless Networks and Communications, 2007. CrownCom 2007. 2nd International Conference on*, pp. 367–372, 2007.
9. J. M. Kim, S. H. Sohn, N. Han, G. Zheng, Y. M. Kim, and J. K. Lee, "Cognitive radio software testbed using dual optimization in genetic algorithm," in *Cognitive Radio Oriented Wireless Networks and Communications, 2008. CrownCom 2008. 3rd International Conference on*, pp. 1–6, 2008.
10. S. Iellamo, L. Chen, and M. Coupechoux, "Proportional and double imitation rules for spectrum access in cognitive radio networks," *Computer Networks*, vol. 57, no. 8, pp. 1863 – 1879, 2013.

11. J. Elias, F. Martignon, A. Capone, and E. Altman, "Non-cooperative spectrum access in cognitive radio networks: A game theoretical model," *Computer Networks*, vol. 55, no. 17, pp. 3832 – 3846, 2011.
12. J. De Bruyne, W. Joseph, L. Verloock, C. Olivier, W. De Ketelaere, and L. Martens, "Field measurements and performance analysis of an 802.16 system in a suburban environment," *Wireless Communications, IEEE Transactions on*, vol. 8, no. 3, pp. 1424–1434, 2009.
13. S. B. et al, "Federating wired and wireless test facilities through emulab and omf: the ilab.t use case" in the proceedings of tridentcom 2012," in *Proceedings of TridentCom*, 2012.
14. "Iperf - the TCP/UDP bandwidth measurement tool." `http://iperf.fr/`. [Online; accessed 2013-07-19].
15. "IEEE standard for information technologyTelecommunications and information exchange between systems local and metropolitan area networksSpecific requirements part 11: Wireless LAN medium access control (MAC) and physical layer (PHY) specifications," *IEEE Std 802.11-2012 (Revision of IEEE Std 802.11-2007)*, pp. 1 –2793, 2012.
16. "Libtrace library for trace processing." `http://research.wand.net.nz/software/libtrace.php`. [Online; accessed 2013-07-19].
17. "tcpdump, a powerful command-line packet analyzer." `http://www.tcpdump.org/`. [Online; accessed 2013-07-19].